ANL/IPNS/CP-96944

The Effects of Uranium Oxide High-level Waste on the Structure of Iron Phosphate Glasses

Yaspal Badyal*, Mevlut Karabulut**, Kanishka Marasinghe**, Marie-Louise Saboungi*, Dean Haeffner* & Sarvjit Shastri*
*Argonne National Laboratory, Argonne, IL 60439
**Graduate Center for Materials Research, University of Missouri-Rolla, Rolla, MO 65409

To be published in the Materials Research Society 1998 Fall Symposium Proceedings

The Effects of Uranium Oxide High-level Waste on the Structure of Iron Phosphate Glasses

Yaspal Badyal*, Mevlut Karabulut**, Kanishka Marasinghe**, Marie-Louise Saboungi*, Dean Haeffner* & Sarvjit Shastri*

*Argonne National Laboratory, Argonne, IL 60439

**Graduate Center for Materials Research, University of Missouri-Rolla, Rolla, MO 65409

Abstract

Because of their unusually good chemical durability, iron phosphate glasses are a natural candidate for a nuclear waste disposal glass. We have studied the effects of UO_2 high-level waste on the structure of iron phosphate glasses with both neutron and high-energy x-ray diffraction using the GLAD instrument of the Intense Pulsed Neutron Source and the 1-BM bending magnet beamline of the Advanced Photon Source, respectively. The results of neutron scattering, which is mostly sensitive to correlations involving light atoms i.e. O-O, Fe-O and P-O, suggest the main structural features of the base glass are largely unaffected by the addition of UO_2. The nearest-neighbour P-O, Fe-O and O-O peaks remain at the same position in real space and their intensities scale approximately with concentration. These findings are consistent with the earlier results of Raman scattering and EXAFS on the Fe-*K* edge where in both cases the spectra remain similar to the base glass. High-energy x-ray scattering, which is sensitive to correlations involving the heavier atoms and thus complements the neutron measurements, is also consistent with uranium occupying interstitial sites in the relatively undisturbed base glass structure. However, important questions remain as to the precise local structure and oxidation state of uranium in these glasses.

Introduction

Studies of binary iron phosphate glasses indicate they possess many of the characteristics required of a stable host medium for immobilizing certains kinds of high-level waste (HLW), such as chemical durability, low processing temperature and high waste loading capacity [1]. The enhanced durability compared to phosphate glass is attributed to the greatly reduced proportion of easily hydrated P-O-P bonds linking $(PO_4)^{3-}$ tetrahedral units [2]. Intoducing iron leads to the formation of more hydration resistant Fe-O-P bonds and the overall densification of the glass. Previous studies of the base glass, $40Fe_2O_3$ - $60P_2O_5$, used in this work suggest a structure related to its crystalline counterpart $Fe_3(P_2O_7)_2$ formed by heat treating the base glass. The crystal structure [3] is comprised of a network of $(Fe_3O_{12})^{-16}$ clusters interconnected via $(P_2O_7)^{-4}$ groups, containing voids big enough to host large ions such as Cs and U. Because the glass is less dense than the crystal it is reasonable to expect these interstitial voids remain a part of the glass structure and are able to accomodate waste components. Raman scattering and EXAFS on the Fe-*K* edge supports this view with the spectra remaining little changed from the base glass as uranium is added [4]. In order to properly assess the usefulness of these glasses for HLW disposal it is clearly important to learn more about how the structure of the glass is affected by waste components. This research describes the findings from both neutron and high-energy x-ray diffraction measurements on iron-phosphate glasses loaded with UO_2. Because neutron diffraction is more sensitive to light elements whereas x-rays scatter more strongly from heavier atoms, together they provide complementary information about structure.

Theory

The total scattering, $S(Q)$, from a system containing n types of atom can be considered the sum of partial correlations, $S_{\alpha\beta}(Q)$, from all the distinct atom pairs α,β weighted for concentration, c, and scattering length, $f(Q)$;

$$S(Q) = \frac{\sum_{\alpha=1}^{n} \sum_{\beta=1}^{n} c_\alpha c_\beta f_\alpha(Q) f_\beta(Q) S_{\alpha\beta}}{\left(\sum_{\alpha=1}^{n} c_\alpha f_\alpha(Q) \right)^2} \qquad (1)$$

The contrast in the scattering from using x-rays and neutrons on the same sample arises from the differing scattering lengths, which are dependant on the scattering vector Q in the case of x-rays but uniformly isotropic for neutrons. The real-space total correlation function of interest, $T(r)$ is obtained from the experimental $S(Q)$ by Fourier transformation ;

$$T(r) = 4\pi\rho r + \frac{2}{\pi} \int_0^{Q_{max}} Q[S(Q) - 1] \sin(Qr) dQ \qquad (2)$$

where ρ is the atomic number density and Q_{max} is the upper limit of the $S(Q)$ data.

Experiment

The x-ray diffraction measurements were carried out on the 1-BM bending magnet beamline of the Advanced Photon source (APS) using a Si (111) monochromator crystal set to produce an incident beam of energy 61.332 KeV (wavelength, 0.2022 Å) [5]. The samples were run in flat-plate symmetrical transmission geometry with the scattering measured by a solid-state Ge detector scanning in the vertical plane to minimise polarisation corrections. The data were corrected for attenuation, multiple scattering and Compton using standard programs. The neutron measurements were made on the General Liquids and Amorphous Materials Diffractometer (GLAD) of the Intense Pulsed Neutron Source (IPNS) [6]. In contrast to the x-ray measurements, a pulsed 'white' beam of neutrons covering the wavelength range 0.12 to 3.0 Å was used. The scattered neutrons, as measured by multiple fixed detectors covering the angular range 8 to 125°, were wavelength-sorted using the time-of-flight technique. The data were corrected for dead time, attenuation, multiple scattering and inelasticity effects, again using standard programs.

Results

The results of the neutron and x-ray measurements are summarised in figure 1 which shows the real-space T(r) functions for each of the samples studied (see table 1 for the compositions). First considering only the neutron results, the nearest-neighbour P-O, Fe-O and O-O peaks (labelled in the figure) are readily identifiable and are seen to remain largely unchanged in position and width upon the addition of UO_2. The heights of these peaks scale approximately with concentration implying the areas under the peaks, and hence the coordination numbers, are also little changed. A peak arising from the Fe-P correlation is visible at $r \sim 3.25$ Å. This peak can be identified unambiguously by comparison with the corresponding peak in the x-ray results for the base glass (sample A) since it is at nearly the same position and the approximate size of the feature scales well with the respective neutron and x-ray weighting factors (the latter being about 4 times larger than the former). With increasing UO_2, the Fe-P peak in the neutron T(r) remains clearly visible and seems to diminish proportionately with the decreasing concentration of iron and phosphorus indicating the Fe-O-P cross-links, believed to be essential to the durability of the base glass, persist. The neutron samples all contain the same ratio of iron and phosphate to that of the base glass thus the results can be readily interpreted in terms of the added uranium occupying interstitial sites in the essentialy unmodified network structure of the starting base glass.

Fig. 1 Comparison of neutron and x-ray real-space total correlation functions

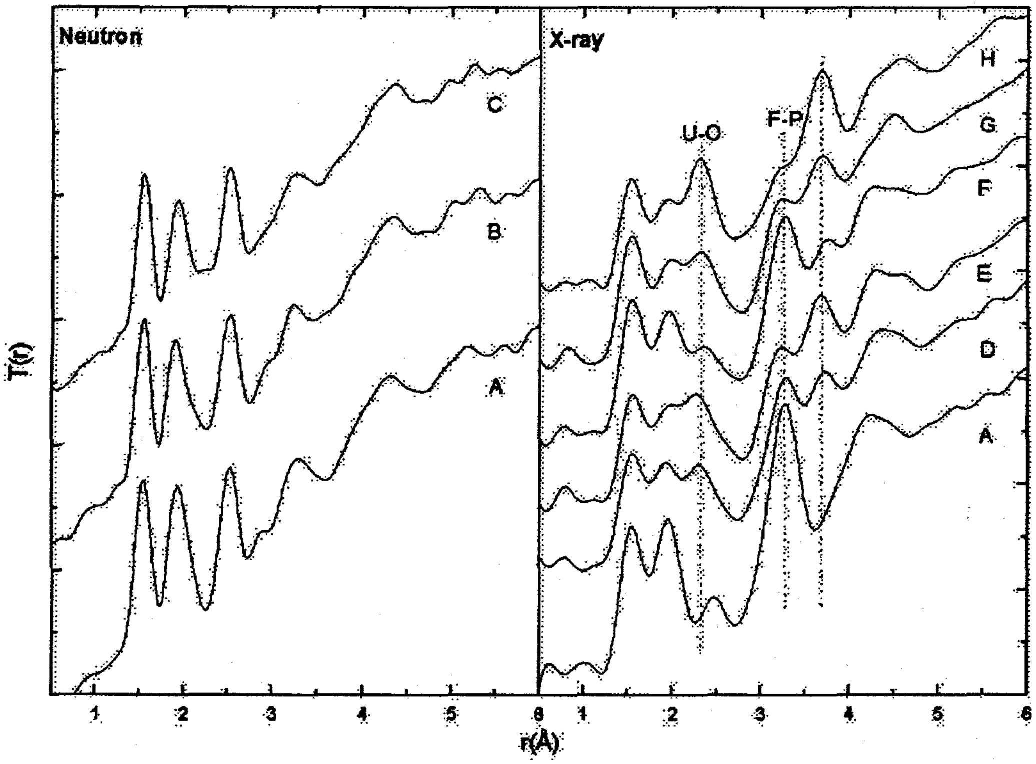

Table 1. Batch composition of the samples studied.

Sample	Batch Composition (mol %)				Fe/P ratio
	Fe_2O_3	Fe_3O_4	P_2O_5	UO_2	
A	40	0	60	0	0.666
B	36	0	54	10	0.666
C	32.4	0	48.6	19	0.666
D	0	27.7	62.3	10	0.666
E	0	26.2	58.8	15	0.666
F	35	0	60	5	0.583
G	30	0	60	10	0.500
H	25	0	60	15	0.416

In contrast to the neutron results, providing information about light atoms, the x-ray results emphasise the scattering from the heavy atoms. In the x-ray T(r), where the nearest-neighbour O-O peak is much less prominent, the addition of UO_2 leads to a steady increase in intensity of an easily identifiable U-O peak at r ~ 2.25 Å. The same peak is apparent as a weak filling-in of the valley between the Fe-O and O-O peaks in the neutron T(r). The height of the P-O peak at r ~ 1.52 Å scales approximately with concentration suggesting the $(PO_4)^{3-}$ tetrahedral units remain unaffected. In addition, the main Fe-O peak at r ~ 1.9 Å clearly decreases as the U-O peak increases, which is to be expected since for the x-ray samples UO_2 was substituted for Fe_2O_3 or Fe_3O_4 i.e. the Fe/P ratio does not remain constant (see table 1). With increasing UO_2, another distinct peak emerges at r ~ 3.6 Å which, given their respective x-ray weighting factors, is probably due to correlations involving U-P and U-Fe rather than U-U.

Figure 2. Base glass neutron/x-ray difference from eliminating the O-O correlation.

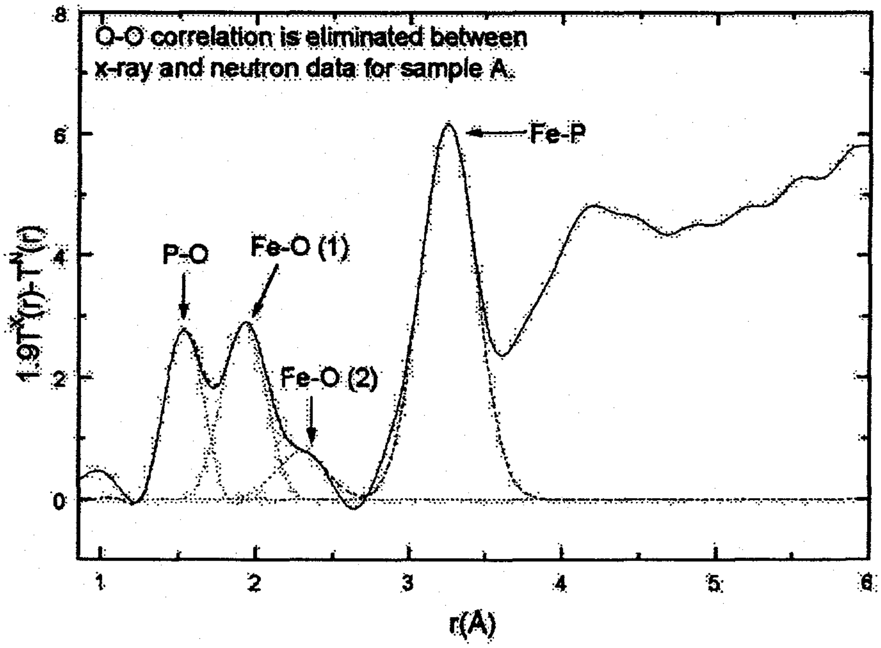

More details about structure can be obtained by first-order differencing of the neutron and x-ray data taking advantage of the contrast in scattering lengths to eliminate at least one of the partial terms in the summation describing the average scattering (see eqn. 1). This can only be done for samples with very similar compositions since the partial pair scattering terms themselves can be expected to change with composition. For the base glass, figure 2 shows the difference T(r) function resulting from elimination of the O-O partial pair correlation term, making it possible to distinguish the Fe-O and Fe-P peaks much less ambiguously. The figure also shows (broken curves) the results of fitting deconvolved gaussians [7] to model the coordination shells for each pair correlation. This gives an average local coordination number for oxygen around phosphorus, $C_p(O)$, of 4.08 which is very close to the ideal value of 4 for regular $(PO_4)^{3-}$ tetrahedra. As for the local environment of Fe, two peaks can be resolved corresponding to short, Fe-O(1), and long, Fe-O(2), bonds with a total coordination number $C_{Fe}(O)$ of 5.82, close to the octahedral coordination expected from the crystal structure of $Fe_3(P_2O_7)_2$. Assuming no contributions from the other pair correlation terms, an *upper limit* for the coordination number $C_{Fe}(P)$ of 4.52 was obtained for the peak labeled Fe-P.

In the case of the uranium-containing glasses, no two identical samples were measured using both neutrons and x-rays although, fortunately, samples B and D have very nearly the same atomic composition so approximate differences can be obtained using these data. Figure 3 shows the difference T(r) from eliminating the O-O term (as was done with figure 2 above for the base glass). The P-O first peak remains at nearly the same position as in the base glass with an estimated coordination number $C_p(O)$ of 4.12 thus confirming the local structure of the $(PO_4)^{3-}$ tetrahedra is not significantly disturbed. Due to overlap with the U-O peak, it is not possible to reliably model the distinct Fe-O(1) and Fe-O(2) peaks seen in the base glass. However, an average coordination number of 5.28 was obtained by fitting a *single* broad gaussian, between two neighbouring gaussians for P-O and U-O, which is consistent with the Fe atoms continuing to occupy octahedral sites. Although it is difficult to estimate a coordination number from the peak labeled Fe-P (due to overlap with other peaks) the presence of a clear peak at the same position as in the base glass seems to confirm the persistence of Fe-O-P bonds.

Figure 3. UO_2 glass neutron/x-ray difference from eliminating the O-O correlation.

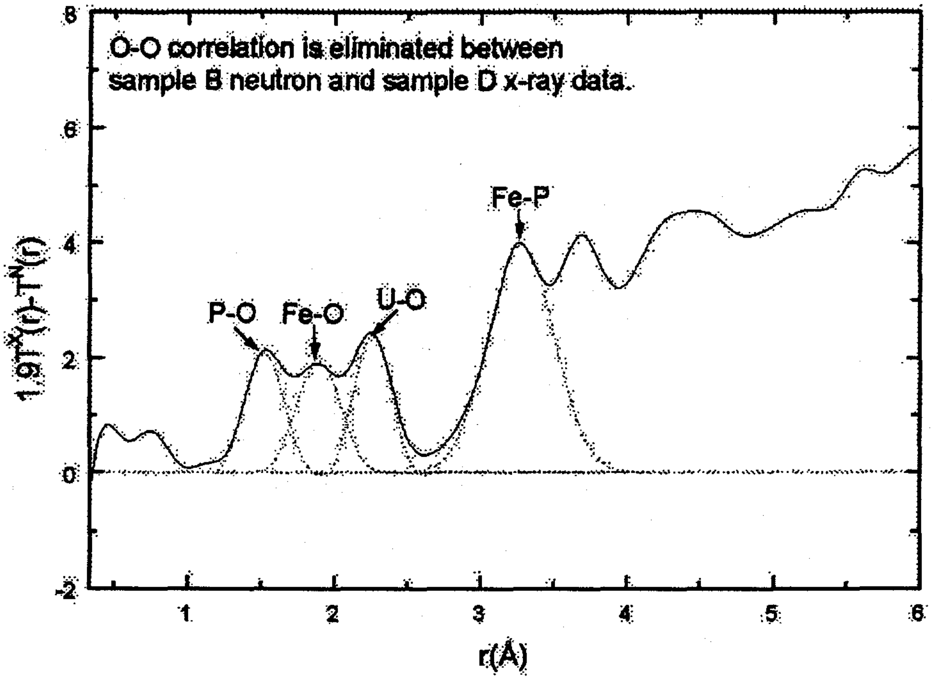

Figure 4. UO_2 glass neutron/x-ray difference from eliminating the Fe-O correlation.

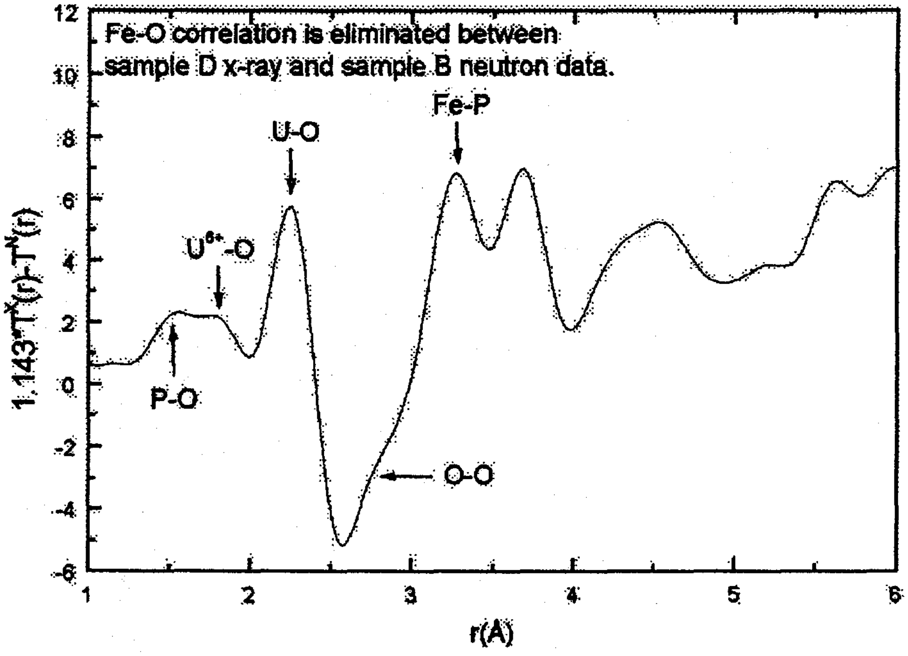

Figure 4 shows the results of eliminating the Fe-O term. Note that due to the order of taking the difference the O-O contribution is negatively weighted hence the inverted main peak for this correlation. In addition to the P-O and U-O peaks clearly visible at the expected positions there appears to be a peak at r ~ 1.8 Å. Although this feature could be a spurious artefact (for example, due to Fourier termination ripple) it may, alternatively, represent a second, shorter, U-O distance typical of uranium in the U^{6+} uranyl ion configuration sometimes found in layered silicate glasses [8]. Dissolved uranium in water is generally found in the hexavalent oxidation state as the divalent uranyl ion UO_2^{2+} whereas U^{4+} is relatively immobile due to the much lower solubility of uranous phases. The question of the oxidation state of uranium is thus directly relevant to the practical usage of these glasses for high-level waste disposal. To learn more about the local order and valence state of uranium in these glasses further work is needed and a combination of uranium edge XANES and EXAFS measurements is suggested.

Conclusions

The effects of uranium oxide high-level waste on the structure of iron phosphate glasses has been studied by complementary neutron and high-energy x-ray diffraction measurements. The data are consistent with the uranium being incorporated into interstitial sites in the essentially unmodified network structure of the starting base glass. These findings are in agreement with the earlier results of Raman scattering and Fe-*K* edge EXAFS where the spectra do not change significantly from the base glass. Differencing of the neutron and x-ray data for a 10 mol% UO_2 glass suggests the intriguing possibility of a U^{6+} uranyl ion configuration although further work is needed to establish the precise local structure and valence state of uranium in these glasses.

Acknowledgements

This work was supported by the Divison of Materials Science, Office of Basic Energy Sciences, US Department of Energy, under Contract W-31-109-ENG-38. We thank the facility staff of the Intense Pulsed Neutron Source and the Advanced Photon Source, Argonne, for their assistance.

References

[1] G.K. Marasinghe, M. Karabulut, C.S. Ray, D.E. Day, M.G. Shumsky, W.B. Yellon, C.H. Booth, P.G. Allen & D.K. Shuh, J. Non. Cryst. Solids, **222**, 144-152 (1997)

[2] G.N. Greaves, S.J. Gurman, L.F. Gladden, C.A. Spence, P. Cox, B.C. Sales, L.A. boatner & R.N. Jenkins, Philos. Mag. B, **58**, 217 (1988)

[3] M. Ijjaali, G. Venturini, R. Geradin, B. Malaman, C. Gleitzer, Eur. J. Solid State Inorg. Chem., **28**, 983 (1991)

[4] G.K. Marasinghe *et al*, Ceramic Transactions, vol 93, expected publication April 1999

[5] H.F. Poulsen, J. Neuefeind, H.-B. Neumann, J.R. Schneider & M.D. Zeidler, J. Non-Cryst. Solids, **188**, 63-74 (1995)

[6] A.J.G. Ellison, R.K. Crawford, D.G. Montague, K.J. Volin & D.L. Price, J. Neut. Research, **1**(4), 61-70 (1993)

[7] S. Susman, K.J. Volin, D.G. Montague & D.L. Price, J. Non. Cryst. Solids, **125**, 168 (1990)

[8] G.S. Knapp,B.W. Veal,D.J. Lam,A.P. Paulikas & H.K. Pan,Materials Letters,**2**(4),253 (1984)